Knee Surgery, Sports Traumatology, Arthroscopy (KSSTA)

Title: Stress on the Posteromedial Region of the Proximal Tibia Increased Over Time after Anterior Cruciate Ligament Injury

Soya Miura. M.D.[1], Koji Iwasaki. M. D., Ph. D.[2], Eiji Kondo. M. D., Ph. D.[3], Kaori Endo. M. D., Ph. D.[1], Shinji Matsubara. M. D., Ph. D.[1], Masatake Matsuoka. M. D., Ph. D.[1], Tomohiro Onodera. M. D., Ph. D.[1], Norimasa Iwasaki. M. D., Ph. D.[1]

1. Department of Orthopaedic Surgery, Faculty of Medicine and Graduate School of Medicine, Hokkaido University, Sapporo, Japan
2. Department of Functional Reconstruction for the Knee Joint, Faculty of Medicine, Hokkaido University, Sapporo, Japan
3. Centre for Sports Medicine, Hokkaido University Hospital, Sapporo, Japan

Corresponding author

- Koji Iwasaki, MD, PhD.
- Institutional address: North-15, West-7, Sapporo, Hokkaido 060-8638, Japan
- Phone: +81-11-706-5934
- Email: kojiwasaki@pop.med.hokudai.ac.jp

Declarations:

- **Conflict of interest:** The institution of an author (KI) has received funding from Olympus terumo biomaterials CORP.
- **Ethical approval:** This study protocol was approved by the institutional review board of Hokkaido university hospital (IRB number, 017-0163).
- **Authors' contribution:** SM collected the data, made the analysis and drafted the work. KI conducted this study, supervised the data analysis and completed the draft. SM, MM supported the data collection. KE advised the CT analysis. EK, OT and NI interpreted the data and revised the draft critically.

Abstract

Purpose Anterior cruciate ligament (ACL) injury induces anterior and rotatory instability of the knee. However, the effect of this instability on the stress distribution in the knee joint in living participants is not clear. The aim of this study was to compare the distribution pattern of subchondral bone density across the proximal tibia in the knees with and without ACL injury, and to investigate the correlation between the distribution patterns of the subchondral bone density and the duration of ACL-deficiency.

Methods Radiographic and computed tomography (CT) data pertaining to 20 patients with unilateral ACL injury without combined injury (ACL-deficient group) and 19 nontraumatic subjects (control group) were collected retrospectively. Subchondral bone density of the proximal tibia was assessed using CT-osteoabsorptiometry. Both the medial and lateral compartments of the proximal tibia were divided into three subregions of equal width in the sagittal direction. The percentage of high subchondral bone density areas (HDA%) in each subregion was quantitatively analyzed.

Results HDA% of the posteromedial region was significantly higher in the ACL-deficient group (mean: 21.6%) than in the control group (14.7%) ($p = 0.002$). In contrast, HDA% of the anteromedial region was significantly lower in the ACL-deficient group (9.4%) than in the control group (15.3%) ($p = 0.048$). The logarithm of the time elapsed from

ACL injury to CT examination showed a significant correlation with HDA% in the posteromedial region ($p = 0.032$).

Conclusions Subchondral bone density in the posteromedial region significantly increased after ACL injury and correlated with the duration of ACL-deficiency in semi-log manner in meniscus intact knees. The increase in stress on the posteromedial region after ACL injury, which induces a change in the subchondral bone density, justifies early ACL reconstruction after ACL injury.

INTRODUCTION

Anterior cruciate ligament (ACL) injury induces anterior and rotatory instability of the knee, which affects the performance level of athletes; moreover, this instability may cause knee buckling or giving way even in non-athletes. Anterior and rotatory instability is known to alter the positional relationship between the distal femur and the proximal tibia [4, 11, 26, 28, 34, 43]. This instability after ACL injury is believed to lead to abnormal stress distribution across the knee joint [6, 9, 12, 42]. In cadaveric studies, the contact stress on the posteromedial part of the proximal tibial articular surface in response to anterior tibial load was found to be higher in ACL-deficient knee than in the intact knee [6, 42]. In addition, the location of the common dynamic stress distribution on the proximal tibial articular surface changed after ACL transection during simulated gait [9].

However, it is technically challenging to measure the actual stress distribution across the knee joint in the ACL-deficient knee. Moreover, whether and how the actual in vivo stress distribution changes after ACL injury is not well characterized.

Computed tomography (CT)-osteoabsorptiometry is an analytical method for in vivo assessment of the stress distribution at joints through the subchondral bone density. It has been demonstrated by our previous studies that CT-osteoabsorptiometry is a useful method for evaluation of in vivo stress distribution in various joints [15, 19-21, 23, 32,

45 33].

46 It was hypothesized that the stress distribution pattern of the proximal tibial
47 articular surface would change over time after ACL injury. The purpose of this study was
48 (1) to compare the distribution pattern of subchondral bone density across the proximal
49 tibia with and without ACL injury, and (2) to clarify the influence of the duration of ACL
50 deficiency on the distribution of subchondral bone density. Using CT-osteoabsorptiometry,
51 the change in stress distribution within each compartment of the proximal tibia after ACL
52 injury and the influence of the time elapsed after ACL injury on the stress distribution
53 across the knee joint could be elucidated by this study.

54

55 **MATERIAL AND METHODS**

56 This study protocol was approved by the institutional review board of Hokkaido
57 University Hospital (IRB number, 017-0163). Analysis was conducted by retrospectively
58 evaluating the preoperative CT scans of the knees of patients who underwent ACL
59 reconstruction between 2016 and 2019 at our institution. Inclusion criteria were patients
60 who had unilateral ACL injury and had undergone CT and MRI examination prior to ACL
61 reconstruction. The exclusion criteria were: (1) meniscal injury which was found in
62 preoperative MRI images (≥ grade II, according to Lotysch and Mink's MRI evaluation

system [29]) or that was diagnosed by arthroscopic examination during the ACL reconstruction surgery; (2) cartilage injury (≥International Cartilage Repair Society [ICRS] grade II [8, 18]); (3) osteoarthritis (≥ Kellgren-Laurence [KL] grade II [24]); (4) concomitant chondral injury or ligament injury detected by preoperative MRI or arthroscopic evaluation; (5) age >35 years (Figure 1). In total, 70 patients were diagnosed with ACL injury during the study's data collection period at our institution. Of those, 50 patients were excluded, and the remaining 20 patients were included in the study as those having ACL-deficient knees (ACL-deficient group) (Figure 1). In addition, for comparison of ipsilateral knee trauma, we collected the data of patients undergoing simultaneous radiographic and CT examinations of the bilateral knees between 2015 and 2019; these patients were considered control subjects. Inclusion criteria for the control group were: (1) osteoarthritis (KL grade ≤ 1) in the contralateral knee, (2) age <35 years at the time of CT, and (3) no trauma history. Nineteen uninjured contralateral knees were used as controls. There were no significant differences in age, sex, HKA angle, PTS angle, and Tegner activity scale score between the control and ACL-deficient groups (Table 1).

Clinical and radiological evaluation

In the ACL-deficient group, the side-to-side differences of the anterior laxity were

measured with a KT-2000 arthrometer (MED metric, San Diego, CA, USA) at 30° of knee flexion under an anterior drawer force of 133 N. For radiological evaluation, bilateral standing anteroposterior (AP), lateral views of the knee, and full-length AP radiographs of the whole lower limb in full extension were assessed. Tibiofemoral osteoarthritis was evaluated according to the KL grading system, Hip-knee-ankle (HKA) angle, and posterior tibial slope (PTS) angle. The PTS was defined as the angle between the line perpendicular to the mid-diaphysis of the tibia and the posterior inclination of the medial tibial plateau. Patient activity before ACL injury was evaluated using the Tegner activity scale [40].

Computed tomography–osteoabsorptiometry

A high-resolution helical CT scanner (Aquilion One/ViSION Edition; Toshiba Medical Systems, Japan) was used to acquire axial images of the knee in full extension. Slice thickness and interval were set at 0.5 mm. The acquired CT data were transferred to a personal computer. The sagittal and coronal slices at 1.0-mm intervals and 3-D bone models were generated from axial CT data using a commercial software (Ziocube®; Ziosoft, Inc., Tokyo, Japan). The sagittal and coronal axes were determined with reference to the epicondylar axis of the distal femoral condyle in the axial slice. By referring to sagittal and coronal CT images and a 3-D CT image of the articular surface of the

proximal tibia, an outline of the medial and lateral compartment of the proximal tibial articular surface was manually selected to include the entire subchondral bone layer of the articular surface in all slices [20]. Subsequently, the subchondral bone density of each generated sagittal slice was analyzed using an original non-commercial software (OsteoDens 4.0) developed at our institution [15, 19, 20, 23, 32, 33]. The maximum increment point in Hounsfield units from the joint surface was set as the starting point of the region of interest, and the maximum point in Hounsfield units was selected automatically in the 2.5-mm region of interest from the starting point [20]. We determined the radiodensity of the identified subchondral bone region at each coordinate point at 1.0-mm intervals. Subsequently, a two-dimensional image that mapped the distribution of subchondral bone density was obtained by stacking the sagittal slices (Figure 2A, 2B). The differences between the maximum and minimum values (in Hounsfield units [HU]) on the mapping images were categorized into nine grades; subsequently, a surface mapping image was generated using these grades to produce a color scale in which red and violet indicated the greatest and lowest bone densities, respectively. The selected areas of the medial and lateral plateaus included the cortical bone at the periphery of the articular surface because it was impossible to exclude the cortical bone using the software. However, these features were manually removed from the target area of analysis in the

117 subsequent quantitative analysis [20].

118 Quantitative analysis of the obtained mapping data focused on the location of the
119 high-density area (HDA) of the articular surface. The HDA was defined as the region
120 containing the coordinate points representing the top 30% area of HU values in each
121 medial or lateral compartment. The medial compartment of the proximal tibia was divided
122 into three subregions of equal width in the sagittal direction, denoted anteromedial (AM),
123 centromedial (CM), and posteromedial (PM) from anterior to posterior. The lateral
124 compartment was similarly divided into anterolateral (AL), centrolateral (CL), and
125 posterolateral (PL) from anterior to posterior (Figure 2C). The percentage of each
126 subregion represented by the HDA (HDA%) was calculated (see Supplemental File). The
127 measurement results in this study are presented to one decimal place of precision.
128 Quantitative analysis was performed in a blinded manner by two observers (## and ##).
129 The same set of images was measured by each examiner after 4 weeks. The averages of
130 these measurements were used in our analysis.

131 The reproducibility of data was evaluated using OsteoDens 4.0 software. Intra-
132 and interobserver reliability were assessed using three randomly selected knees from the
133 control group and ACL-deficient group. HDA% was measured independently by two
134 observers (KI and SM) in these six knees; a total of 36 subregions were measured twice

in a blinded manner at 4-week intervals. The intraclass correlation coefficients for intraobserver reliability were 0.88 (KI) and 0.91 (SM), respectively, and the intraclass correlation coefficient for interobserver reproducibility was 0.87.

Statistical analysis

Statistical analyses were performed using JMP Pro 14.0 (SAS Institute Inc., Cary, NC, USA). $P < 0.05$ was considered statistically significant. Comparisons between control and ACL-deficient groups were performed using the Student's *t* test or the chi-square test. Pearson's correlation coefficient was used to examine the relationship between HDA% in each subregion and other variables, including anterior laxity, period from ACL injury to CT, HKA angle, and PTS angle, because they are believed to influence the distribution of subchondral bone density [22, 36, 41] or the biomechanics of the knee joint [3, 35]. Post hoc power analysis revealed that for an alpha value of 0.05, a power of 0.96 on a sample size of 20 knees was achieved for the difference in HDA% in the PM region.

RESULTS

HDA% in each subregion

HDA% of the posteromedial region in the ACL-deficient group was 7% higher than in

153 the control group (p = 0.002). In contrast, HDA% of the anteromedial region in the ACL-
154 deficient was 6% lower than in the control group (p = 0.048). There were no significant
155 differences in HDA% of centromedial region and subregions of the lateral compartment
156 between the ACL-deficient and control groups (Table 2).
157
158 **Correlation between HDA% and other variables**
159 HDA% of the posteromedial region showed no correlation with the time elapsed from
160 ACL injury to CT examination (n.s., r = 0.288), but showed a significant correlation with
161 the logarithm of the time elapsed from ACL injury to CT examination (p = 0.032. r =
162 0.480) (Figure 3). HDA% of the anteromedial region showed no correlation with the time
163 elapsed either on the arithmetic plot or the semi-log plots. HDA% of the posteromedial
164 region showed no correlation with other variables, including anterior laxity, HKA angle,
165 and PTS angle.
166
167 **DISCUSSION**
168 The main findings of the present study were that HDA% of the posteromedial region of
169 the proximal tibia in the ACL-deficient group with intact meniscus was significantly
170 higher than that in the control group Furthermore, HDA% of the posteromedial region

showed a significant correlation with the duration of ACL-deficiency on semi-log curves.

Previous studies involving CT-osteoabsorptiometry have indicated that the distribution pattern of subchondral bone density reflects the distribution of the stress acting on the joint surface under actual loading conditions [19-21, 23, 31-33]. Funakoshi et al. found high-stress distribution patterns on the anterolateral part of the capitellum and the anterolateral part of the ulna in symptomatic patients with ulnar collateral ligament insufficiency [15]. Therefore, CT-osteoabsorptiometry can help assess the *in vivo* stress distribution across the ACL-deficient knee joint. In the present study, HDA% in the posteromedial region of the proximal tibia was found to be higher in the ACL-deficient knees than in the normal knees. This result suggests that ACL injury increased the stress on the posteromedial region of the proximal tibia, since the changes in subchondral bone density are believed to result from changes in stress distribution. Experimental studies using animal models, ACL transection induced progression of osteoarthritis over time [1, 7, 13]. These results suggested that chronic ACL-deficiency leads to accumulation of stress, which causes the initiation and progression of osteoarthritis (OA) [5]. These speculations were supported by our findings in the present study.

There was a positive correlation between the logarithm of the time elapsed since ACL-deficiency and HDA% of the posteromedial region in the meniscus intact knees.

189 These results suggested that stress on the posteromedial region increased rapidly after
190 ACL injury and was accumulated gradually over time, while the meniscus was intact.
191 These findings suggested that patients with ACL injury should undergo ACL
192 reconstruction as soon as possible from the perspective of aggressive prevention of
193 osteoarthritis, even though the meniscus was not injured.

194 There are several potential mechanisms of the changes in stress distribution after
195 ACL injury including anterior translation of the tibia relative to the femoral condyle [11,
196 26, 28, 42] and anterolateral rotatory instability [11, 26, 34, 42]. Furthermore, three-
197 dimensional gait analyses revealed reduced internal rotational moment in ACL-deficient
198 knees during the terminal stance phase. This gait pattern was described as a “pivot-shift
199 avoidance gait” [14, 38]. Theoretically, anterior translation is believed to increase the
200 stress on the posteromedial region of the tibial plateau and decrease the stress on the
201 anteromedial region because of the concave shape of the medial tibial plateau. In addition,
202 internal rotatory instability may decrease the stress on the posteromedial region of the
203 tibial plateau and increase the stress on the anteromedial region. “Pivot shift avoidance
204 gait” may affect reciprocally compared to rotatory instability. This study suggested that
205 ACL injury increased the stress on the posteromedial region without any correlation with
206 the extent of anterior instability and PTS; in addition, ACL injury led to decreased stress

207 on the anteromedial region. Taking into account both the assumed mechanisms affecting
208 the stress distribution and the obtained results in the anteromedial and posteromedial
209 region, anterior translation is believed to be the main mechanism of the altered stress
210 distribution. Furthermore, internal rotation may not counteract the effect of anterior
211 translation on the stress distribution, or "pivot shift avoidance gait" may play an important
212 role in the stress distribution compared to internal rotation after ACL injury.

213 A quasi-static and dynamic biomechanical cadaveric study revealed increase of
214 dynamic contact stress on the posterior lateral tibial plateau [9], indicating that the
215 posterior tibial plateau hit against lateral femoral condyle when tibia rotated internally. In
216 the present study, we found no evidence of increased stress on the posterior lateral tibial
217 plateau. CT-OAM method indicated the resultant stress through the distribution pattern
218 of subchondral bone density across the joint, reflecting all movements including not only
219 walking but the compensatory movement against internal rotatory instability. Thus, these
220 differences in the speculation of the stress distribution between the dynamic
221 biomechanical cadaveric study and this CT-OAM study demonstrated a compensatory
222 movement against rotatory instability, which could not be simulated by the knee simulator
223 [9].

224 Leg alignment has been reported to strongly influence the distribution of

subchondral bone density between the medial and lateral compartments of the proximal tibia [2, 17, 41], indicating that leg alignment counteracted a change in the distribution of subchondral bone density in the sagittal direction due to knee instability. Our previous study demonstrated that the relative value of subchondral bone density in eight sub-regions in the coronal direction among subjects increased significantly, up to 6%, and shifted laterally after high tibial osteotomy (HTO) [20]. Therefore, in the present study, we used the relative value of bone density within compartments in the sagittal direction to detect a change in subchondral bone density distribution in the sagittal direction after ACL injury. Consequently, there was a 5% decrease in the relative value of bone density, compared with the control group, in the anteromedial region and an increase of 6% in the posteromedial region after ACL injury, demonstrating a rearward shift of subchondral bone density distribution. Taking into account the drastic change in knee biomechanics before and after HTO, 5%–6% differences in the relative value of bone density in the sagittal direction between ACL-deficient and control groups was thought to be a substantial change. Although clinical evaluation was not performed in this study, the rearward shift of stress distribution, which induced the rearward shift of subchondral bone density distribution, has been reported to be a cause of the high incidence of medial meniscus injury in chronically ACL-deficient knees [16, 39].

In addition to leg alignment, patient activity level and PTS angle could have affected bone density. ACL injuries tend to affect individuals with a high activity level, which could have an impact on bone density [30, 37], and PTS angle was associated with knee instability in ACL-deficient knees [10]. However, there were no significant differences in the activity level and PTS angle between the control and ACL-deficient groups in our study. Therefore, those factors may not have contributed to the difference between the ACL-deficient and control groups.

Regarding the influence of the initial injury itself on the bone density, ACL injury is usually provoked by internal rotation and anterior translation, resulting mainly in bone bruising at the posterior wall of the lateral tibial plateau [25, 43]. The posterior wall of the lateral tibial plateau is outside the region of interest in the CT-OAM method. The metaphyseal part of the proximal tibia is too deep to assess by CT-OAM. Furthermore, HDA% of the posterolateral region was not significantly changed in the ACL-deficient group compared to that in the control group. Thus, initial injury may not influence the distribution of subchondral bone density assessed by the CT-OAM method.

In addition, the effect of any instability immediately after ACL injury on subchondral bone density might be minimal; however, in a previous study, a 10% decrease in the absolute BMD of the proximal tibia was seen 100 days after ACL injury

with reduced mobility and low activity [27]. Our results of a significant change in the relative value of subchondral bone density in the posteromedial region 90 days after ACL injury may be supported by this change in absolute BMD after ACL injury.

Some limitations of our study should be considered when interpreting the findings. First, the stress was not measured directly but through the distribution of subchondral bone density based on the CT-OAM findings [31]. Furthermore, the absolute value of BMD was not evaluated; instead, the relative value in each subregion of each compartment was evaluated. It should be noted that the stress distribution evaluated by the CT-OAM method may not reflect the actual stress. Second, this study lacked a standardized rehabilitation protocol and level of rest. Despite these limitations, the strength of this study was that we matched the two groups with respect to factors that may influence the distribution pattern of subchondral bone density (including age, BMI, and geometry of knee). Thus, a basic clarification that in vivo stress distribution changes over time after ACL surgery is demonstrated by our results.

CONCLUSION

It has been demonstrated that HDA of the posteromedial region of the proximal tibia in ACL-deficient knees was significantly higher than that in ACL-intact knees. Moreover, it

was found that HDA of the posteromedial region was correlated with the duration of ACL deficiency on semi-log plots. The increase in stress on the posteromedial region over time after ACL injury, which induces a change in the subchondral bone density, provides orthopedic surgeons with a justification for early ACL reconstruction after ACL injury.

Acknowledgements

We would like to thank Enago (www.enago.jp) for editing a draft of this manuscript.

REFERENCES

1. Adams ME, Brandt KD (1991) Hypertrophic repair of canine articular cartilage in osteoarthritis after anterior cruciate ligament transection. J Rheumatol 18:428-435
2. Akamatsu Y, Koshino T, Saito T, Wada J (1997) Changes in osteosclerosis of the osteoarthritic knee after high tibial osteotomy. Clin Orthop Relat Res 334:207-214
3. Andriacchi TP, Briant PL, Bevill SL, Koo S (2006) Rotational changes at the knee after ACL injury cause cartilage thinning. Clin Orthop Relat Res 442:39-44
4. Andriacchi TP, Dyrby CO (2005) Interactions between kinematics and loading during walking for the normal and ACL deficient knee. J Biomech 38:293-298
5. Andriacchi TP, Mundermann A (2006) The role of ambulatory mechanics in the initiation and progression of knee osteoarthritis. Curr Opin Rheumatol 18:514-518
6. Bedi A, Chen T, Santner TJ, El-Amin S, Kelly NH, Warren RF, et al. (2013) Changes in dynamic medial tibiofemoral contact mechanics and kinematics after injury of the anterior cruciate ligament: a cadaveric model. Proc Inst Mech Eng H 227:1027-1037
7. Brandt KD, Braunstein EM, Visco DM, O'Connor B, Heck D, Albrecht M (1991) Anterior (cranial) cruciate ligament transection in the dog: a bona fide model of osteoarthritis, not merely of cartilage injury and repair. J Rheumatol 18:436-446
8. Brittberg M, Winalski CS (2003) Evaluation of cartilage injuries and repair. J Bone Joint Surg Am 85-A Suppl 2:58-69
9. Chen T, Wang H, Warren R, Maher S (2017) Loss of ACL function leads to alterations in tibial plateau common dynamic contact stress profiles. J Biomech 61:275-279
10. Dejour D, Pungitore M, Valluy J, Nover L, Saffarini M, Demey G (2019) Preoperative laxity in ACL-deficient knees increases with posterior tibial slope and medial meniscal tears. Knee Surg Sports Traumatol Arthrosc 27:564-572
11. Dennis DA, Mahfouz MR, Komistek RD, Hoff W (2005) In vivo determination of normal and anterior cruciate ligament-deficient knee kinematics. J Biomech 38:241-253
12. Du PZ, Markolf KL, Boguszewski DV, McAllister DR (2018) Femoral Contact Forces in the Anterior Cruciate Ligament Deficient Knee: A Robotic Study. Arthroscopy 34:3226-3233
13. Fischenich KM, Button KD, Coatney GA, Fajardo RS, Leikert KM, Haut RC, et al. (2015) Chronic changes in the articular cartilage and meniscus following traumatic impact to the lapine knee. J Biomech 48:246-253
14. Fuentes A, Hagemeister N, Ranger P, Heron T, de Guise JA (2011) Gait adaptation in chronic anterior cruciate ligament-deficient patients: Pivot-shift avoidance gait. Clin Biomech (Bristol, Avon) 26:181-187
15. Funakoshi T, Furushima K, Momma D, Endo K, Abe Y, Itoh Y, et al. (2016) Alteration of Stress

Distribution Patterns in Symptomatic Valgus Instability of the Elbow in Baseball Players: A Computed Tomography Osteoabsorptiometry Study. Am J Sports Med 44:989-994

16. Hagino T, Ochiai S, Senga S, Yamashita T, Wako M, Ando T, et al. (2015) Meniscal tears associated with anterior cruciate ligament injury. Arch Orthop Trauma Surg 135:1701-1706

17. Han X, Cui J, Xie K, Jiang X, He Z, Du J, et al. (2020) Association between knee alignment, osteoarthritis disease severity, and subchondral trabecular bone microarchitecture in patients with knee osteoarthritis: a cross-sectional study. Arthritis Res Ther 22:203

18. Hjelle K, Solheim E, Strand T, Muri R, Brittberg M (2002) Articular cartilage defects in 1,000 knee arthroscopies. Arthroscopy 18:730-734

19. Irie T, Takahashi D, Asano T, Arai R, Terkawi MA, Ito YM, et al. (2018) Is There an Association Between Borderline-to-mild Dysplasia and Hip Osteoarthritis? Analysis of CT Osteoabsorptiometry. Clin Orthop Relat Res 476:1455-1465

20. Iwasaki K, Kondo E, Matsubara S, Matsuoka M, Endo K, Yokota I, et al. (2021) Effect of High Tibial Osteotomy on the Distribution of Subchondral Bone Density Across the Proximal Tibial Articular Surface of the Knee With Medial Compartment Osteoarthritis. Am J Sports Med 49:1561-1569

21. Iwasaki N, Minami A, Miyazawa T, Kaneda K (2000) Force distribution through the wrist joint in patients with different stages of Kienbock's disease: using computed tomography osteoabsorptiometry. J Hand Surg Am 25:870-876

22. Johnston JD, Masri BA, Wilson DR (2009) Computed tomography topographic mapping of subchondral density (CT-TOMASD) in osteoarthritic and normal knees: methodological development and preliminary findings. Osteoarthritis Cartilage 17:1319-1326

23. Kameda T, Kondo E, Onodera T, Iwasaki K, Onodera J, Yasuda K, et al. (2021) Changes in the Contact Stress Distribution Pattern of the Patellofemoral Joint After Medial Open-Wedge High Tibial Osteotomy: An Evaluation Using Computed Tomography Osteoabsorptiometry. Orthop J Sports Med 9:2325967121998050

24. Kellgren JH, Lawrence JS (1957) Radiological assessment of osteo-arthrosis. Ann Rheum Dis 16:494-502

25. Kim-Wang SY, Scribani MB, Whiteside MB, DeFrate LE, Lassiter TE, Wittstein JR (2021) Distribution of Bone Contusion Patterns in Acute Noncontact Anterior Cruciate Ligament-Torn Knees. Am J Sports Med 49:404-409

26. Kondo E, Merican AM, Yasuda K, Amis AA (2010) Biomechanical comparisons of knee stability after anterior cruciate ligament reconstruction between 2 clinically available transtibial procedures: anatomic double bundle versus single bundle. Am J Sports Med 38:1349-1358

27. Kroker A, Besler BA, Bhatla JL, Shtil M, Salat P, Mohtadi N, et al. (2019) Longitudinal Effects of Acute Anterior Cruciate Ligament Tears on Peri-Articular Bone in Human Knees Within the

First Year of Injury. J Orthop Res 37:2325-2336

28. Kvist J (2004) Sagittal plane translation during level walking in poor-functioning and well-functioning patients with anterior cruciate ligament deficiency. Am J Sports Med 32:1250-1255

29. Lotysch M, Mink J, Crues JV, Schwartz SA (1986) Magnetic resonance imaging in the detection of meniscal injuries. Magn Reson Imaging 4:185

30. Momma D, Iwamoto W, Endo K, Sato K, Iwasaki N (2020) Stress Distribution Patterns Across the Shoulder Joint in Gymnasts: A Computed Tomography Osteoabsorptiometry Study. Orthop J Sports Med 8:2325967120962103

31. Muller-Gerbl M, Putz R, Hodapp N, Schulte E, Wimmer B (1989) Computed tomography-osteoabsorptiometry for assessing the density distribution of subchondral bone as a measure of long-term mechanical adaptation in individual joints. Skeletal Radiol 18:507-512

32. Nishida K, Iwasaki N, Fujisaki K, Funakoshi T, Kamishima T, Tadano S, et al. (2012) Distribution of bone mineral density at osteochondral donor sites in the patellofemoral joint among baseball players and controls. Am J Sports Med 40:909-914

33. Onodera T, Majima T, Iwasaki N, Kamishima T, Kasahara Y, Minami A (2012) Long-term stress distribution patterns of the ankle joint in varus knee alignment assessed by computed tomography osteoabsorptiometry. Int Orthop 36:1871-1876

34. Scarvell JM, Smith PN, Refshauge KM, Galloway HR, Woods KR (2004) Comparison of kinematic analysis by mapping tibiofemoral contact with movement of the femoral condylar centres in healthy and anterior cruciate ligament injured knees. J Orthop Res 22:955-962

35. Schatka I, Weiler A, Jung TM, Walter TC, Gwinner C (2018) High tibial slope correlates with increased posterior tibial translation in healthy knees. Knee Surg Sports Traumatol Arthrosc 26:2697-2703

36. Sharma L (2001) Local factors in osteoarthritis. Curr Opin Rheumatol 13:441-446

37. Shiota J, Momma D, Yamaguchi T, Iwasaki N (2020) Long-term Stress Distribution Patterns Across the Ankle Joint in Soccer Players: A Computed Tomography Osteoabsorptiometry Study. Orthop J Sports Med 8:2325967120963085

38. Takeda K, Hasegawa T, Kiriyama Y, Matsumoto H, Otani T, Toyama Y, et al. (2014) Kinematic motion of the anterior cruciate ligament deficient knee during functionally high and low demanding tasks. J Biomech 47:2526-2530

39. Tashiro Y, Mori T, Kawano T, Oniduka T, Arner JW, Fu FH, et al. (2020) Meniscal ramp lesions should be considered in anterior cruciate ligament-injured knees, especially with larger instability or longer delay before surgery. Knee Surg Sports Traumatol Arthrosc 28:3569-3575

40. Tegner Y, Lysholm J (1985) Rating systems in the evaluation of knee ligament injuries. Clin Orthop Relat Res 198:43-49

41. Wada M, Maezawa Y, Baba H, Shimada S, Sasaki S, Nose Y (2001) Relationships among bone

mineral densities, static alignment and dynamic load in patients with medial compartment knee osteoarthritis. Rheumatology (Oxford) 40:499-505

42. Wang D, Kent RN, 3rd, Amirtharaj MJ, Hardy BM, Nawabi DH, Wickiewicz TL, et al. (2019) Tibiofemoral Kinematics During Compressive Loading of the ACL-Intact and ACL-Sectioned Knee: Roles of Tibial Slope, Medial Eminence Volume, and Anterior Laxity. J Bone Joint Surg Am 101:1085-1092

43. Willinger L, Athwal KK, Williams A, Amis AA (2021) An Anterior Cruciate Ligament In Vitro Rupture Model Based on Clinical Imaging. Am J Sports Med 49:2387-2395

FIGURE LEGENDS

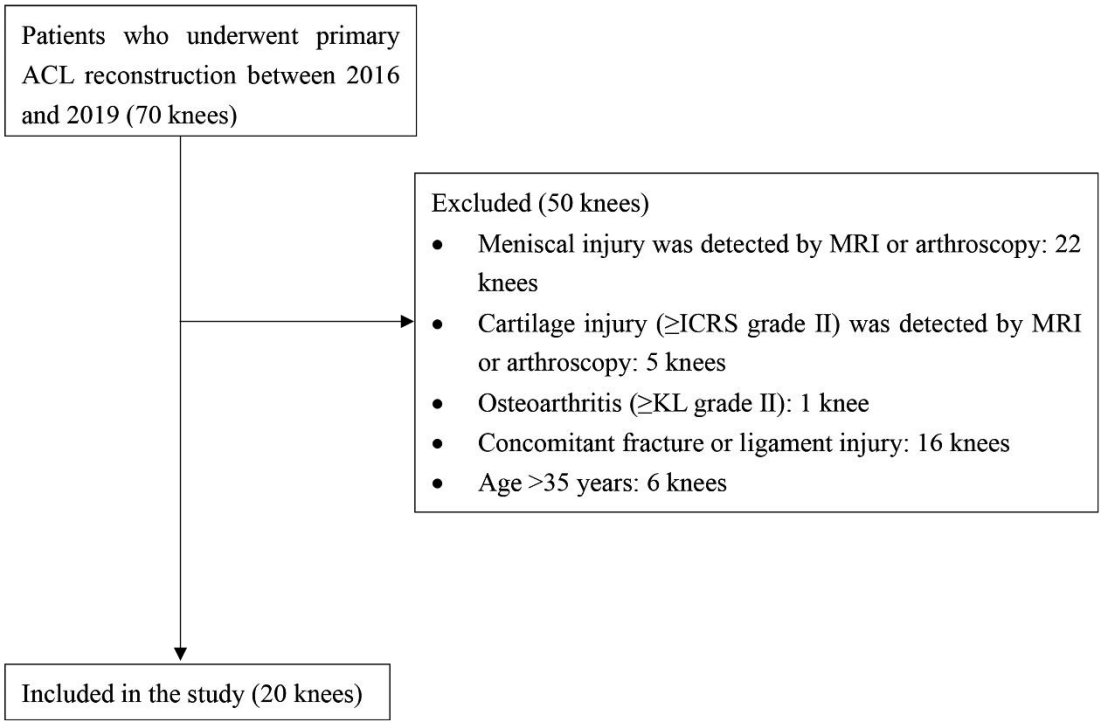

Figure 1. Flowchart of study enrollment. ICRS, International Cartilage Regeneration & Joint Preservation Society-Cartilage Repair Assessment system; KL, Kellgren-Laurence.

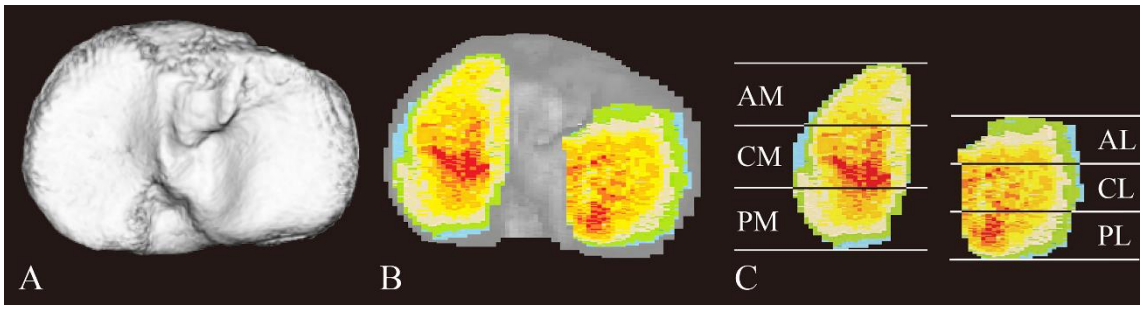

Figure 2. Identification of the subchondral bone regions of the proximal tibia using a customized software. (A, B) The subchondral bone density of the selected region was automatically measured at each coordinate point in each 1.0-mm sagittal slice. (C) Both the medial and lateral compartments of the tibial articular surface were divided into three

412 subregions each from anterior to posterior for quantitative analysis of the distribution of

413 high subchondral bone density area

414 AM, anteromedial; CM, centromedial; PM, posteromedial; AL, anterolateral; CL,

415 centrolateral; PL, posterolateral

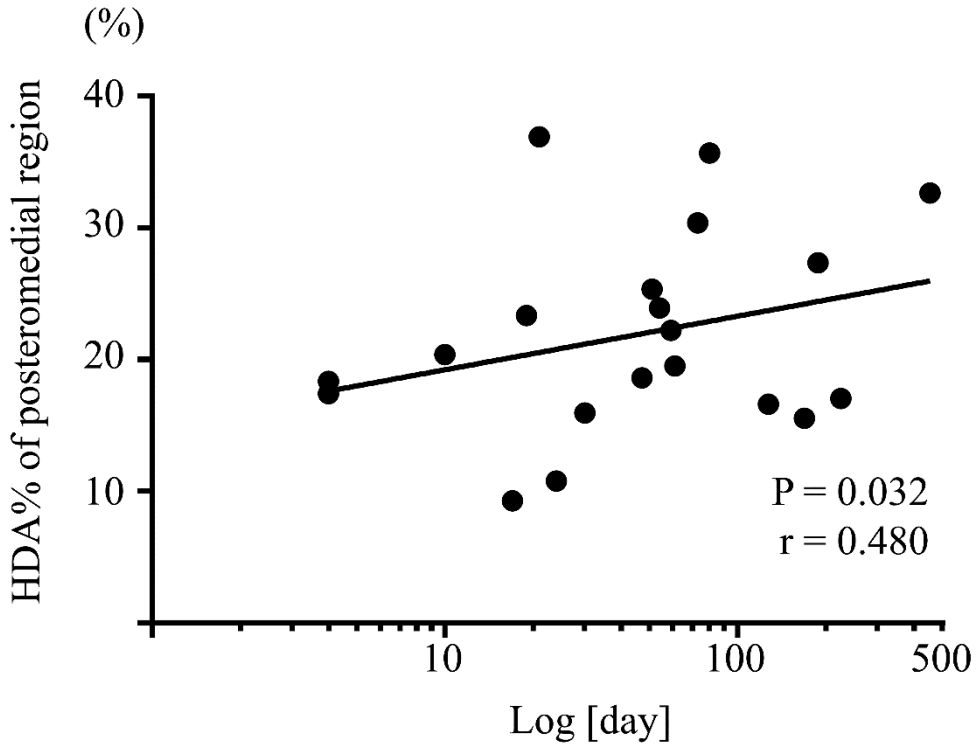

416

417 **Figure 3.** Semi-log plots of the time elapsed from ACL injury vs. HDA% in the

418 posteromedial region of the proximal tibia

419 ACL, anterior cruciate ligament; HDA%, percentage of high subchondral bone density

420 area

421

422 **Table 1. Characteristics of the study population**[a]

	Control group (n = 19)	ACLD group (n = 20)	*p* value
Age, years	23.4 (21.3–26.5)	21.5 (18.5–23.6)	n.s.
Male:Female, n	10:9	10:10	n.s.
BMI, kg/m^2	24.1 (21.8–26.5)	24.3 (22.3–26.2)	n.s.
Anterior laxity, mm	n/a	3.2 (1.8–4.5)	n/a
Period from ACL injury to CT examination, days	n/a	91.4 (35.8–146.9)	n/a
HKA angle, degrees	−0.5 (−2.6–1.6)	−0.3 (−1.8–1.3)	n.s.
PTS angle, degrees	10.4 (8.6–12.2)	10.7 (8.9–12.5)	n.s.
Tegner activity scale score	6.9 (6.1–7.7)	6.4 (5.5–7.2)	n.s.

[a]Data presented as frequency or mean (95% confidence interval).

ACL, anterior cruciate ligament; ACLD, anterior cruciate ligament deficient; Anterior laxity: side-to-side anterior knee laxity at 30° flexion, BMI, body mass index; CT, computed tomography; HKA, hip-knee-ankle; n/a, not applicable; n.s., not significant; PTS, posterior tibial slope.

Table 2. Quantitative analysis of HDA% in each subregion[a]

		Control group	ACLD group	*p* value
Medial compartment (%)	AM	15.3 (9.6–21.0)	9.4 (6.8–12.0)	0.048
	CM	52.0 (47.8–56.3)	52.4 (49.3–55.5)	n.s.
	PM	14.7 (12.5–17.0)	21.6 (18.0–25.3)	0.002
Lateral compartment (%)	AL	3.1 (1.2–5.0)	2.7 (1.3–4.1)	n.s.
	CL	38.2 (34.6–41.9)	38.9 (36.4–41.4)	n.s.

	PL	43.1 (38.4–47.8)	44.7 (40.2–49.1) n.s.

[a]Data presented as mean (95% confidence interval)

ACLD, anterior cruciate ligament deficient; AL, anterolateral; AM, anteromedial; CL, centrolateral; CM, centromedial; HDA%, percentage of high subchondral bone density area; n.s., not significant; PL, posterolateral; PM, posteromedial.